Electronic Supplementary Material (ESI) for Journal of Materials Chemistry A.
This journal is © The Royal Society of Chemistry 2015

Supporting information for

A POM-Organic Framework Anode for Li-Ion Battery

Yanfeng Yue,*[a,b] Yunchao Li,[a,c] Zhonghe Bi,[a] Gabriel M. Veith,[d] Craig A. Bridges,[a] Bingkun Guo,[a] Jihua Chen,[e] David R. Mullins,[a] Sumedh P. Surwade,[a] Shannon M. Mahurin,[a] Hongjun Liu,[a] M. Parans Paranthaman,[a,c] and Sheng Dai*[a, f]

[a]Chemical Sciences Division, Oak Ridge National Laboratory, Oak Ridge, Tennessee 37831, USA
[b]Department of Biology, Geology, and Physical Science, Sul Ross State University, Alpine, Texas 79832, USA
[c]The Bredesen Center for Interdisciplinary Research and Graduate Education, University of Tennessee, Knoxville, Tennessee 37996, USA
[d]Materials Science and Technology Division, Oak Ridge National Laboratory, Oak Ridge, Tennessee 37831, USA
[e]Center for Nanophase Materials Sciences, Oak Ridge National Laboratory, Oak Ridge, Tennessee 37831, USA
[f]Department of Chemistry, University of Tennessee, Knoxville, Tennessee 37996, USA

Containing the following details:

1. Experimental and measurement details
2. Powder XRD patterns
3. Thermal gravimetric analysis of as-made POMOF-1
4. FT-IR curve of as-made POMOF-1
5. Cyclic voltammograms (CVs) of POMOF-1
6. Cycling performance at a current density of 0.25 C
7. Powder XRD patterns of POMOF-1 before and after battery cycling
8. Cycling performance of ligand BDC
9. Cycling performance of $Na_9[A\text{-}\alpha\text{-}PW_9O_{34}]\cdot nH_2O$
10. Ni 3p XPS spectrum

1. Experimental and characterizations

1.1 Experimental details

1.1.1 Materials

Synthesis of $Na_9[A\text{-}\alpha\text{-}PW_9O_{34}]\cdot nH_2O$ was prepared by a literature method.[1] The nickel(II) chloride hexahydrate (FW: 248.86), 1,4-benzenedicarboxylic acid (H_2BDC), ethylenediamine (en), sodium acetate, and glacial acetic acid were obtained from Aldrich and used without further purification.

1.1.2 Synthesis of POMOF-1

POMOF-1: A sample of $Na_9[A\text{-}\alpha\text{-}PW_9O_{34}]\cdot nH_2O$ (0.30 g) and $NiCl_2\cdot 6H_2O$ (0.80 g) was stirred in a 0.5M sodium acetate buffer (pH 4.8, 10 mL) for 5 min, forming a green clear solution. Then 0.30 mL was added drop wise with continuous stirring. To this solution, H_2BDC (0.20 g) was added and stirred for 120 min. The resulting solution was sealed in a 35-mL stainless steel reactor with a Teflon liner and heated at 170 °C for 5 days, and then cooled to room temperature, after which green prismatic crystals were obtained. The resulting product was dried under vacuum at 60 °C overnight before FT-IR, TGA, powder XRD, TEM, nitrogen adsorption-desorption, and battery characterization.

1.2 Characterizations

1.2.1 Fourier Transform Infrared Spectroscopy (FT-IR). The FT-IR spectrum of the as made POMOF-1 was recorded by an attenuated total reflection Fourier transform infrared (ATR-FTIR) spectrophotometer (Perkin-Elmer Spectrum One, Perkin-Elmer Co., USA). The spectra were averaged over 16 scans at 4 cm^{-1} resolution obtained in the range of 650–4000 cm^{-1}.

1.2.2 Thermogravimetric analysis (TGA). Thermogravimetric analysis (TGA) was carried out by using a TA Instrument 2950 from room temperature to 800 °C at a heating rate of 5 °C min^{-1} under air atmosphere.

1.2.3 Powder X-ray Diffraction (XRD). Powder x-ray diffraction (XRD) analysis was used to confirm the crystallinity as well as the phase purity of the bulk materials. Powder XRD patterns were recorded on a PANalytical Empyrean diffractometer equipped with Cu Kα radiation (λ = 1.5406 Å). Data for the material "as made" were collected in reflection geometry, and typically between 5° to 80° 2θ. Data for the desolvated sample were collected in transmission mode with the sample contained between two mylar sheets to minimize absorption of moisture, typically between 3.5^o to 85° 2θ. The mylar sheets were sealed with Torr Seal epoxy such that moisture transmission only occurred through the film.

1.2.4 Gas Adsorption Analysis. Gas adsorption studies were done to confirm the permanent porosity of the as-synthesized composite sample as well as to determine the surface area. Low pressure gas adsorption experiments were performed on a Micromeritics Tristar 3000 analyzer at 77 K. Around 100 mg as made POMOF-1 was evacuated for 6 hours at 150 °C and subsequently loaded for adsorption analysis.

1.2.5 Transmission Electron Microscopy (TEM). Electron diffraction and TEM experiments were examined with a Zeiss Libra 120 at 120 kV. An emission current as low as 5μA and minimal exposure times were used to effectively reduce electron-beam-induced sample damage, along with frequent morphology monitoring. Selected area electron diffraction experiments used an aperture size of about 1 micron in diameter and the obtained

diffraction patterns were calibrated against a thin film gold standard, assuming the d spacing of Au (111) planes is 0.235 nm.

1.2.6 X-ray photoelectron spectroscopy (XPS).

Surface chemistry was probed using a PHI 3056 XPS spectrometer with Al *K*α radiation (1486.6 eV) at a measurement pressure below 10^{-9} Torr. The samples were disassembled in an Ar-filled glovebox and rinsed with anhydrous dimethyl carbonate (Sigma-Aldrich) and transferred under vacuum directly to the XPS sample chamber using an airtight transfer device. High-resolution scans were acquired at 350 W with 23.5 eV pass energy and 0.05 eV energy step. The energy scale of the spectra was calibrated to the C1s peak at 284.8 eV.

1.2.7 Electrochemical Experiments. Electrochemical experiments were carried out using coin cells. The battery electrode mixtures consisted of 65 wt % active materials, 20 wt % super C45 and 15 wt % polyvinylidene fluoride (PVDF). These materials were ground together by hand and then dispersed in NMP to form a slurry. Slurries were deposited on copper foils, and dried at 80 °C for 6 hours, and then further dried under vacuum overnight at 110 °C. The loading of active materials was 1.2 – 1.5 mg cm^{-2}. The cells were assembled using 1M $LiPF_6$ in EC/DEC/DMC 1:1:1 vol % electrolyte. The charge experiment was conducted using Land CT2001A with current density of 400 mA/g.

1.2.8 X-ray absorption spectroscopy (XAS).

The experiments were recorded at the Ni k edge (8333 eV) and the W L_{III} edge (10204 eV) on Beamline X19a at the National Synchrotron Light Source. An Si(111) double crystal monochromator was used and detuned by 30% to reject higher harmonics. The x-ray absorption was measured in transmission. Ion chambers for measuring I_o and I_t were filled with nitrogen and a 50:50 mixture of N_2: Ar, respectively. The samples (before/after Li-ion battery cycling) were ground to a fine powder and spread on Kapton tape, which was then folded to produce a uniform thickness and an absorbance, μ(x), of approximately 0.3–0.5. The photon energies were calibrated and aligned by mounting Ni or W foils downstream of the samples.

The programs ATHENA and ARTEMIS (available through the DEMETER software package, version 0.9.17) were used to reduce and fit the data, respectively.[2] Data reduction consisted of pre-edge subtraction, background determination, normalization and spectral averaging.

1.2.9 Raman spectrum.

The Raman measurements were carried out using a Renishaw 1000 Raman spectrometer equipped with a 514.5 nm Ar-ion laser, which was focused onto the sample with a 50× objective lens.

Reference

[1] A. P. Ginsberg, *Inorganic Syntheses*, *Vol. 27*, Wiley, New York, 1990, p.85.
[2] B. Ravel, M. Newville, *J Synchrotron Radiat.*, 2005, *12*, 537.

2. PXRD patterns of as-made and desolvated POMOF

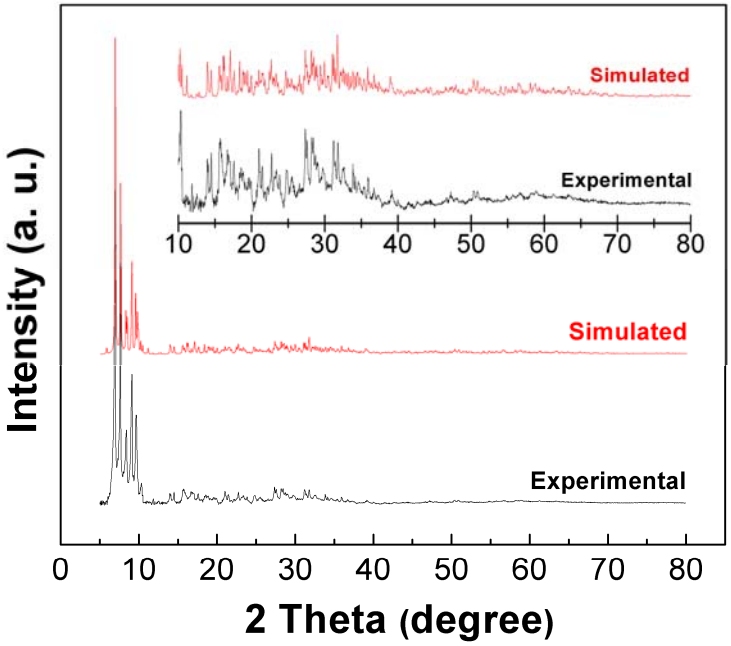

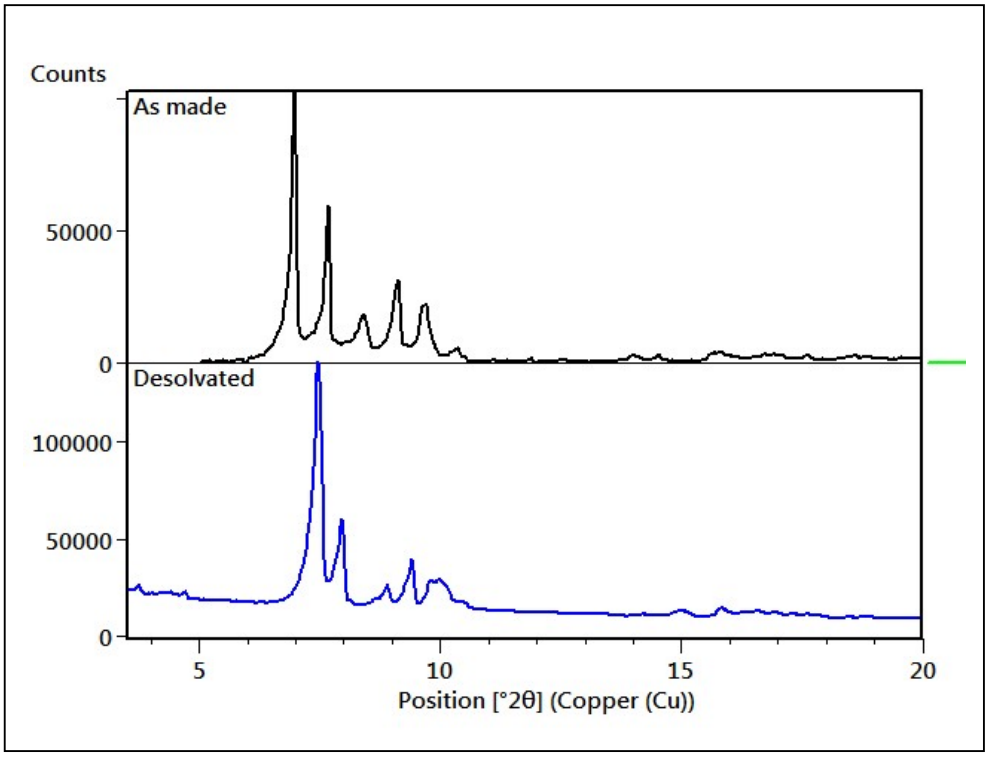

Figure S1a. Top: PXRD patterns of as-made POMOF-1 and simulated pattern from Cambridge Structural Database (CSD) crystal structure information. The simulated pattern appears very similar to the experimental data. Bottom: PXRD patterns of the desolvated form show similarities to the as-made POMOF-1, with a peak shift to smaller d-spacings indicating a smaller cell volume. Additional peaks are seen below 5° 2θ in the desolvated form that disappear upon resolvation (rehydration) in air. Attempts to index and solve the structure of the desolvated form are under way.

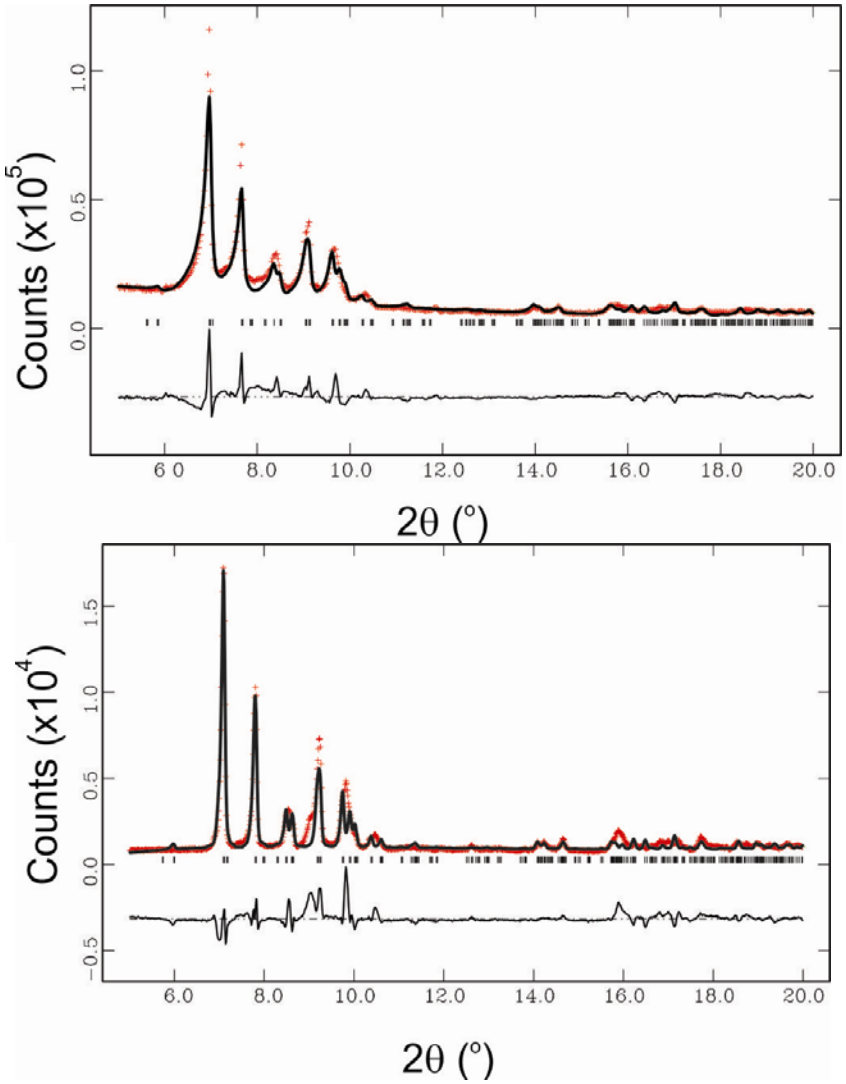

Figure S1b. Top: Rietveld refinement of as-made POMOF-1 against the reported single crystal structure (CCDC 668400) in space group P-1 with lattice parameters refined to *a*=12.771(1)Å, *b*=19.730(2)Å, *c*=25.391(7)Å, α = 87.56(1)°, β = 89.86(1)°, γ = 79.64(1)°, V= 6288(1) Å^3. The fit quality was low, with χ^2=48, and wR_p=9.66. The refinement reveals both the presence of an impurity (peaks in the difference pattern) and chemical inhomogeneity (causing the apparently broad peak asymmetry), which are not evident from simple comparisons with simulated spectra. The peak asymmetry suggests that a gradient exists in the filling of pores with solvent, resulting in a spread of lattice parameters and indicating that the derived lattice parameters represent an average. Bottom: Rietveld refinement of the desolved form after rehydration in air. The peaks are sharpened relative to the as-made form due to more homogeneous pore filling, and the contribution from a second phase is more clearly evident in the difference pattern (plotted at negative counts, below the calculated [black] and observed [red] patterns). Data were refined in space group P-1 with lattice parameters refined to *a*=12.7583(9)Å, *b*=19.756(2)Å, *c*=25.407(1)Å, α = 87.56(1)°, β = 89.77(1)°, γ = 79.70(6)°, V= 6294.7(6) Å^3; data ranged from 5-75° 2θ. The fit quality was improved for the more intense low angle peaks of the main phase, with χ^2=14.54, and wR_p=12.28. Attempts to refine the impurity as a second POMOF-1 phase with the same structure, but different lattice parameters, were not successful. The coincidence of low angle peaks between the impurity and the main phase, along with evidence from XANES, EXAFS and XPS presented in this paper, suggest that the impurity may be a related structure with the local SBU motif retained.

3. Thermal gravimetric analysis of as-made POMOF-1

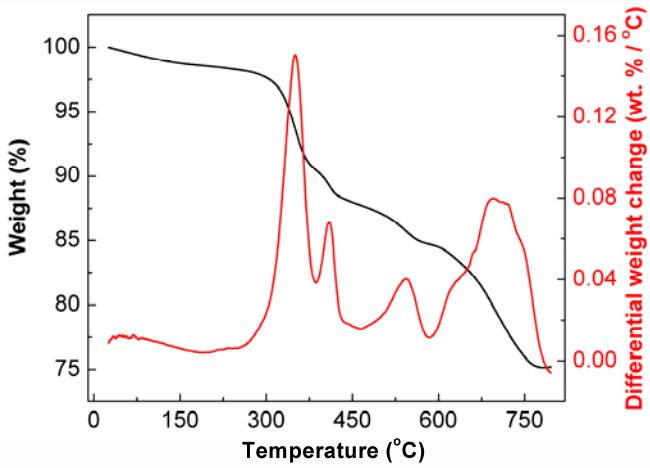

Figure S2. Thermal gravimetric analysis (TGA) under air atmosphere of as-made POMOF-1. TG curve of POMOF-1 shows major weight loss stages in the regions of 50–300, 350–580 and 580–750 ºC, respectively. The weight loss processes are attributed to the loss of water molecules and organic ligands. Assuming that the residue corresponds to WO_3 and NiO, the observed weight loss is in agreement with the calculated value (17.7 %).

4. FT-IR measurements

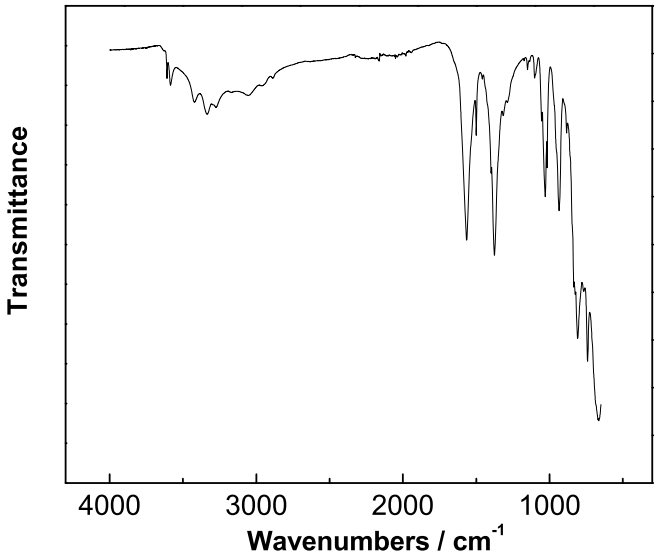

Figure S3. FT-IR spectrum of as-made POMOF-1.

5. Cyclic voltammetry curves

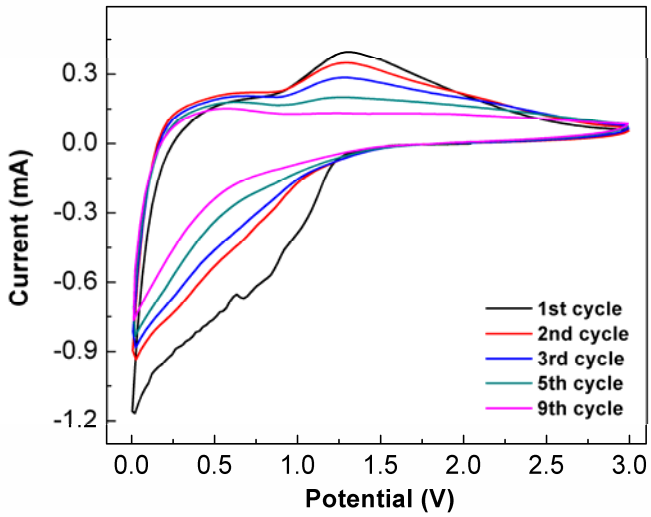

Figure S4. Cyclic voltammetry (CV) curves at a scan rate of 0.2 mV/s.

6. Cycling performance at a current density of 0.25 C

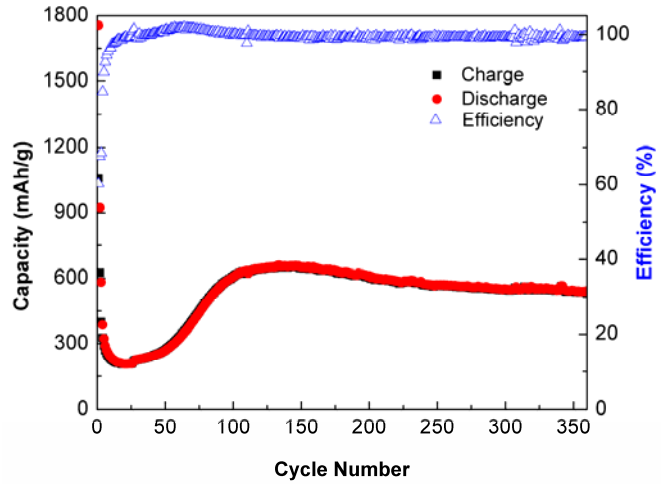

Figure S5. Cycling performance between 5 mV and 3 V vs Li^+/Li at a current density of 0.25 C.

7. Powder XRD patterns of POMOF-1 before and after battery cycling

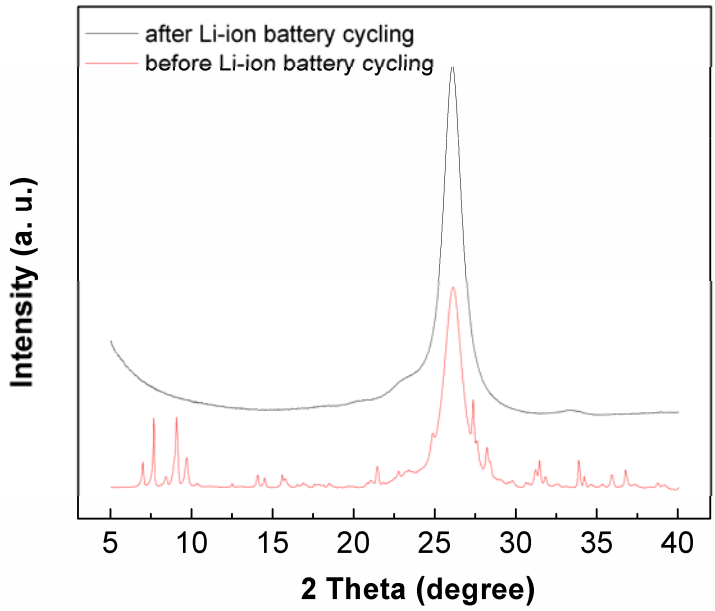

Figure S6. Powder XRD patterns of POMOF-1 before and after battery cycling. The broad, intense peak near 26° 2θ is from the Teflon film. While the POMOF-1 is crystalline before cycling, the structure has become amorphous after cycling.

8. Cycling performance of ligand BDC

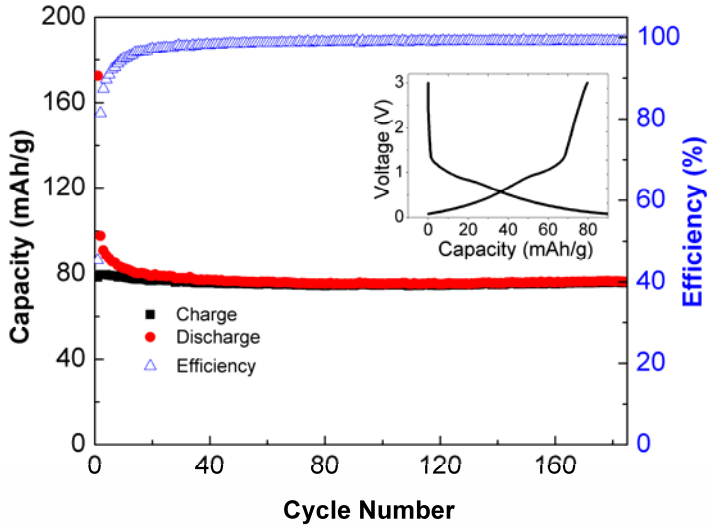

Figure S7. Cycling performance of ligand BDC under a current of 70 mA/g.

9. Cycling performance of $Na_9[A\text{-}\alpha\text{-}PW_9O_{34}]\cdot nH_2O$ at current density of

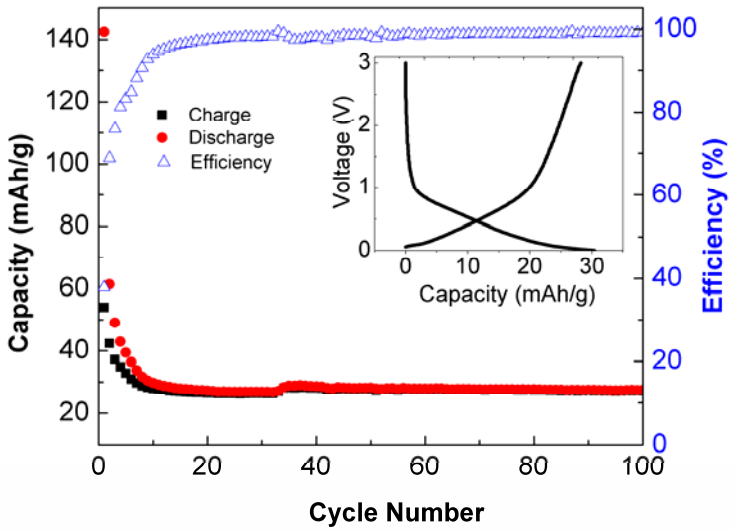

Figure S8. Cycling performance of $Na_9[A\text{-}\alpha\text{-}PW_9O_{34}]\cdot nH_2O$ under a current of 21 mA/g.

10. Ni 3p XPS spectrum

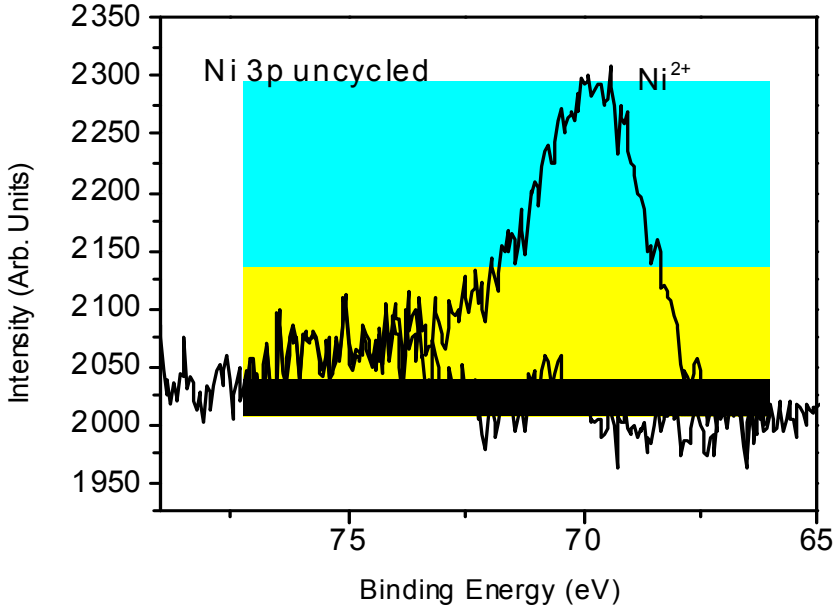

Figure S9. Ni 3p XPS data collected for the uncycled electrode.